Front. Phys., 2011, 6(4): 350–356
DOI 10.1007/s11467-011-0212-1

PERSPECTIVE

A reflection on the contrast between the Cooper pairing in iron-based and conventional superconductors

Fa Wang[1,*], **Dung-Hai Lee**[2,3,†]

[1] *Department of Physics, Massachusetts Institute of Technology, Cambridge, MA 02139, USA*
[2] *Department of Physics, University of California at Berkeley, Berkeley, CA 94720, USA*
[3] *Materials Sciences Division, Lawrence Berkeley National Laboratory, Berkeley, CA 94720, USA*
*E-mail: *wangfa@mit.edu, †dunghai@berkeley.edu*

Received September 6, 2011; accepted September 14, 2011

In this Perspective article we review retrospectively the streamline of our work on iron-based superconductors, and reflect on the mechanism of Cooper pairing in conventional and unconventional, such as iron-based superconductors. The main theme of this review is the concept of effective interaction and renormalization group.

Keywords Cooper pairing, iron-based superconductors, effective interaction, renormalization group

PACS numbers 74.20.Rp, 74.20.Mn, 74.25.Jb, 74.72.Jt

In his article on "Developments of Concepts in Superconductivity" [1], John Bardeen wrote the following passage, "*A derivation from first principles of the effective interaction which gives rise to superconductivity, and thus the critical temperature, is a very difficult task and has not been accomplished for any superconducting element, compound, or alloy.*"

A key word in the above sentences is "the effective interaction". While the Coulomb interaction between charges is the "bare" interaction governing physical phenomena below the energy scale of a few electron volts, the effective interaction that causes the low energy/low temperature ($\lesssim 10$ meV) behaviors of atoms, molecules, or electrons in solids are usually very different in nature.

Let us take the interaction between two helium atoms as an example. The bare interaction includes the Coulomb attraction between the helium nuclei and the electrons, and the Coulomb repulsion between the two nuclei and between the electrons. However, as long as the atoms do not overlap, there is an effective attractive force (the "London dispersion force") between the atoms which is responsible for the liquification of helium below 4.2 Kelvin. The emergence of this attractive interaction involves (1) the screening of the Coulomb interaction due to the formation of helium atoms, and (ii) the effects of virtual polarization. Let us further elaborate on (ii). When two helium atoms approach each other a perturbation on individual atoms is created, so that an off-diagonal matrix element between the ground state and the dipole-moment-possessing first excited state becomes non-zero. As a result, a small dipole moment is induced, which in turn generates the mutual attraction. This is pictorially illustrated in Fig. 1(a). The fact that virtual excitations into high energy levels generate effective interaction between low energy levels is a well known phenomenon in elementary quantum mechanics. For example, let us consider the three energy levels depicted in the left panel of Fig. 1(b). In second order perturbation theory the mixing between the two lower energy levels with the higher energy one causes a shift in the energy of the lower levels as well as induces an "interaction" between them [Fig. 1(b)]. In theoretical jargon this fact is often referred to as the effective interaction generated by integrating out the high energy excitations.

The celebrated BCS theory [2] for conventional superconductors is based on Landau's Fermi liquid conjecture, which states that despite the strong bare Coulomb repulsion, at low energy electrons in a metal behave as non-interacting "quasiparticles". This sets the stage for the meager phonon-mediated attraction to cause the quasiparticles to pair up. The state of Landau's independent quasiparticles is known as the "Fermi liquid" [3]. It is known that Fermi liquids are unstable in exactly one way [4, 5], namely, when an attractive interaction exists between quasiparticles, the Fermi liquid is unstable with respect to the Cooper pair condensate — the superconducting state. The abundance of the superconducting state among different materials is a manifestation of the

©Higher Education Press and Springer-Verlag Berlin Heidelberg 2011

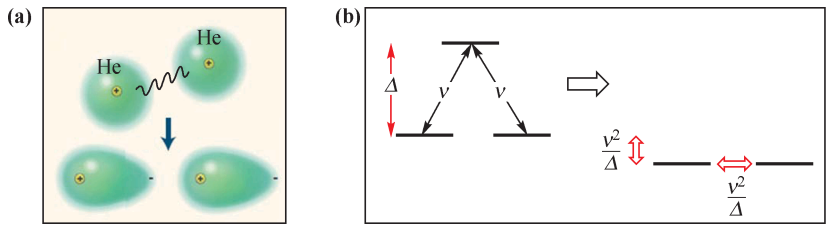


Fig. 1 **(a)** An illustration of the virtual polarization process which generates the attractive interaction between helium atoms. **(b)** A simple example of the generation of effective interaction by integrating out high energy excited states.

fact that over a wide temperature range the Fermi liquid is a common "crossover" state.

Nowadays many strongly correlated materials apparently do not pass through the Fermi liquid before becoming superconducting. The best established case is the cuprate high temperature superconductors [6, 7]. The recently discovered iron-based superconductors [8] might also belong to that category. For example the highest T_c $Ba(Fe_{1-x}Co_x)_2As_2$ compound exhibits "bad metal" behavior [9] where the low temperature resistivity drops linearly with temperature and extrapolate to values much larger than that of ordinary metal [10].

Thus we define conventional superconductors as those materials which go through the Fermi liquid before becoming superconducting. On the contrary, an unconventional superconductor does not pass the Fermi liquid state on its way to superconducting. Of course, we should be cautious in exercising this division, because a wide temperature range (especially at low temperatures) is often required to identify the hallmarks of a Fermi liquid. Often the most important temperature range (the lowest temperatures) is interrupted by superconductivity in high temperature superconductors.

Empirically it is known that in unconventional superconductors there are often other electronic orders competing with superconductivity. The most prominent competitor is often the antiferromagnetism. In nature there are many superconducting compounds which exhibit a similar phase diagram (Fig. 2), where as a functional of a control parameter (chemical doping/substitution, or pressure) the antiferromagnetic phase is replaced by a "superconducting dome". The precise manner by which the antiferromagnetic phase is connected/disconnected to the superconducting phase varies from material to material, but the fact that antiferromagnetic phase is proximate to the superconducting phase is common among all of them. In addition to the antiferromagnetic state there are other electronic instabilities found to compete with superconductivity. For example in the cuprates, uni-directional spin/charge density wave (or stripes) [11, 12] are present in many important cuprate families. At present other prominent competing states include orbital magnetic state which breaks [13] or does not break [14] the lattice translation symmetry, and possibly even certain two-dimensional charge density wave state. For the iron-based superconductors there are increasing evidence that certain electronic instability that breaks the 90° rotation symmetry also competes with the antiferromagnetism and superconductivity [15–17].

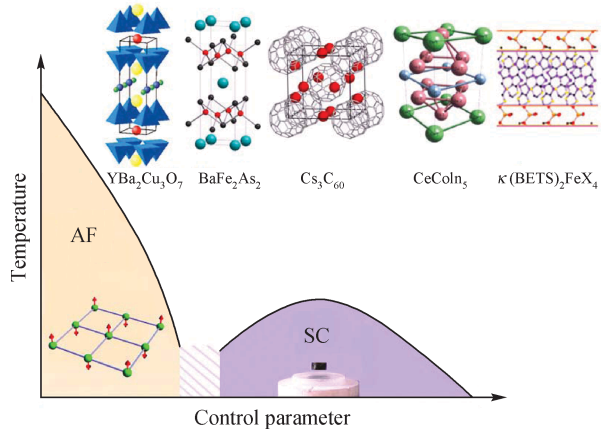


Fig. 2 Five families of compound (the top panel) that show the phase diagram shown in the bottom panel. Here the control parameter is either pressure or chemical doping/substitution. The hatched region hides different ways by which the superconducting and antiferromagnetic phases are connected.

Of course the presence of competing electronic instabilities is consistent with the statement that the normal state is not a Fermi liquid, because as we have stated earlier superconductivity is the only instability of a Fermi liquid. (More precisely we should say superconductivity is the only instability that can be triggered by infinitesimal interaction.) Thus if one imagines "integrating out" more and more high energy excitations and watch how the effective interaction at the lowest energy develops (i.e., a renormalization group calculation) one might encounter a bifurcated process where small change in the initial bare interaction could lead to qualitatively different effective interaction (i.e., they drive very different electronic ordering, or even "topological" order [18]) at the lowest energy (Fig. 3).

Unfortunately such a "dream" calculation cannot be performed at present days. The road block is one that is common to most renormalization group scheme, namely, as the effective interaction develops more and more different types of interaction are generated. The inability to prove the interaction will settle to certain limiting form and find it is where the difficulty lie.

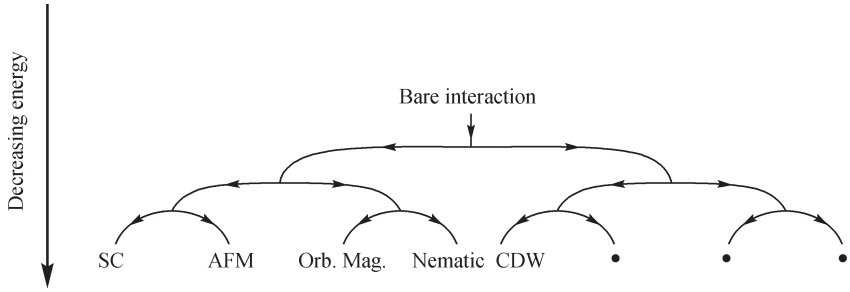


Fig. 3 A schematic illustration of the bifurcation process by which the effective interaction is generated.

In the following we focus our efforts on finding the effective interaction for the iron-based superconductors. Like the cuprates there are many subfamilies among the iron-based superconductors. Four such prominent subfamilies are shown in Fig. 4. The phase diagrams of these materials have quite a bit of variation. Three prominent types of phase diagrams are shown in Fig. 5. The Fermi surfaces of most of the iron-based materials consists of hole pockets near the Brillouin zone center and electron pocket near the zone face [19]. In the early days, motivated by the fermiology [i.e., the geometry of Fermi surfaces (see Fig. 6)] determined by the bandstructure calculation, Mazin *et al.* conjectured that "nesting related AFM spin-density-wave-type spin fluctuations near wave vectors connecting the electron and hole pockets" is the cause of pairing [20]. In addition, owing to the

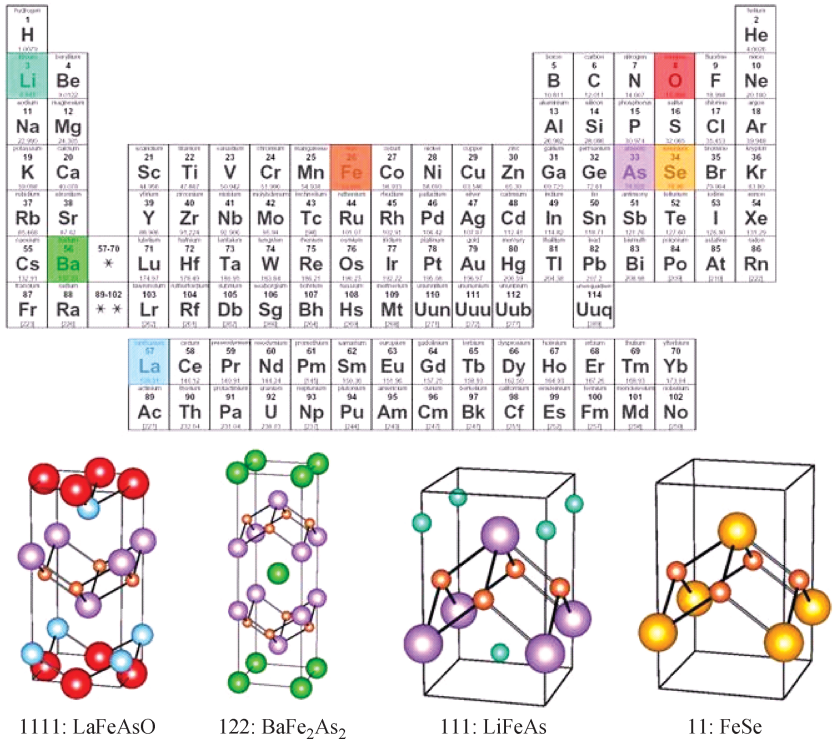


Fig. 4 The structure of the parent compounds in four prominent families of the iron-based superconductors. The constituent chemical elements are shown in the periodic table (color coded).

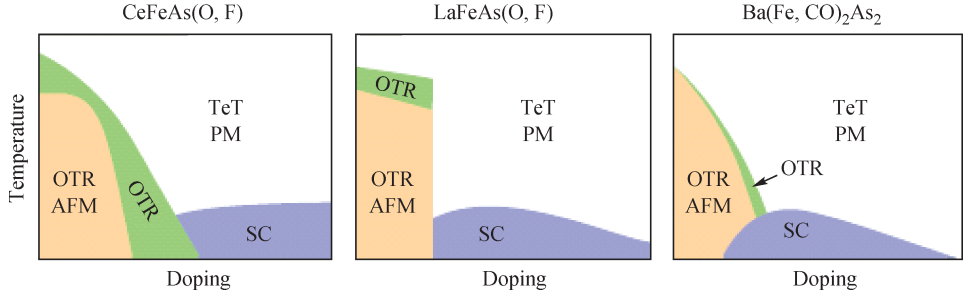


Fig. 5 Three different types of phase diagram for the iron-based superconductors.

repulsiveness of the spin fluctuation mediated pairing, they conjectured that the superconducting order parameter should have opposite sign on the electron (red in Fig. 6) and hole (blue in Fig. 6) Fermi surfaces.

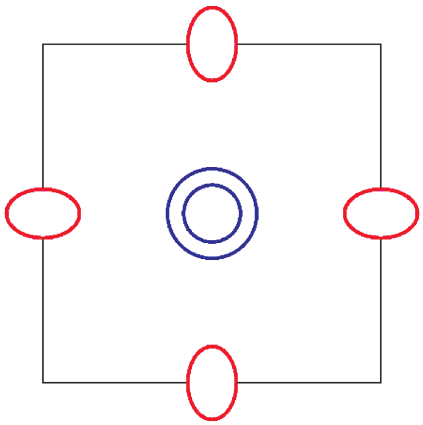


Fig. 6 A schematic representation of a fixed k_z crossection of the Fermi surface of the electron doped 1111 compounds. Blue → hole Fermi surfaces, red → electron Fermi surfaces. The Brillouin zone we use corresponds to that of one iron per unit cell (i.e., the unfolded zone).

Recently the discovery of $K_xFe_{2-y}Se_2$ superconductor families defies this line of reasoning. As shown in Ref. [21] the superconducting phase of the $K_xFe_{2-y}Se_2$ compound show only electron-like Fermi surfaces [22]. The hole Fermi surfaces at the zone center are absent. Later bandstructure and photoemission studies prove the existence of a small 3D electron-like Fermi surface centered at $k_z = \pi$. Thus the fermiology of $K_xFe_{2-y}Se_2$ is completely different from other iron-based superconductors, however, it has a $T_c \sim 30$ K, comparable with other 122 compounds (e.g., $Ba_{1-x}K_xFe_2As_2$).

From the beginning we set our goal to be performing an as un-biased calculation as possible and survey all electronic instabilities. The natural way of achieving this is through some kind of renormalization group calculations. However, it is apparent to us that the strength of electronic correlation in this material is intermediate, making this an extremely difficult task. After a bit of shopping we decided to adopt the "functional renormalization group" (FRG) method developed by Zanchi and Schulz [23] and Honerkamp and Rice [24] for the cuprates. By its nature, FRG is a perturbative approach. It sums all "one loop" diagrams in computing the rate of change of the entire electron–electron scattering function, hence the phrase "functional" RG (which depends on the momenta and spins of the incoming and outgoing electrons) as the cutoff energy is lowered (Fig. 7). (The cutoff energy separates the "integrated" from the "not-yet-integrated" excitations.) It does not assume any subset of scattering process (Feynman diagrams) as more important. Rather, it sums all particle–particle, particle–hole and vertex correction diagrams. Another virtue of FRG is that it can be integrated with realistic bandstructure calculation. Hence the interaction Hamiltonian used in FRG is the part of electron-electron correlation which is not accounted for by the bandstructure (mean-field) theory. Nonethless, FRG is only an one loop perturbative calculation, hence, strictly it is not a controlled approximation in the sense of, say, the ϵ-expansion of Wilson and Fisher [25]. However, one would expect this type of calculation to have a good chance of capturing the right physics when the interaction is weak.

We first performed such a calculation using a two-band model [26], and the results was publicized in the cond-mat archive in the early days. Due to the fact that two bands are not quite adequate in describing the bandstrcuture of the pnictides, we decided to perform the FRG calculation using the realistic five-band bandstructure. That turned out to be quite a challenge, but after some efforts we finished it [27]. Interestingly, as far as pairing is concerned, our early two-band result is qualitatively the same as the later five-band result. Later, in collaboration with H. Zhai we analyzed our FRG results in greater details and found that in addition to pairing and antiferromagnetism, the pnictides have two other types of competing instabilities: Fermi surface distortion and bond-current magnetism [28]. The RG flow for these instabilities and the caricatures of their ordering patterns are shown in Fig. 8. Among the two extra instabilities the Fermi surface distortion is particularly worth mention. We found two types of Fermi surface distortions in close competition. The first type does not break any symmetry. It simply causes both the hole and electron Fermi surfaces to shrink (When it is shrunk sufficiently the electron Fermi surface breaks into disconnected pieces). The other type of Fermi surface distortion breaks the 90° rotation symmetry of the crystal. This Pomeranchuk type distortion is a band version of orbital ordering. It couples to the antiferromagnetism strongly (because the latter also break the 90° rotation symmetry [29]), hence they reinforce each other. This Fermi surface distortion (or orbital ordering) could be closely related to the recent growing evidence of a non-magnetic "nematic" state [15–17]. We have checked that qualitatively the same

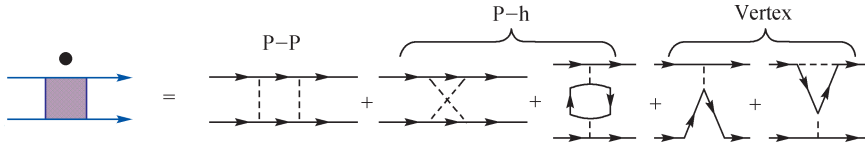


Fig. 7 The Feynman diagrams included in the one-loop functional renormalization group calculation. The left-hand side represents the energy logarithmic derivative of the effective electron–electron scattering function.

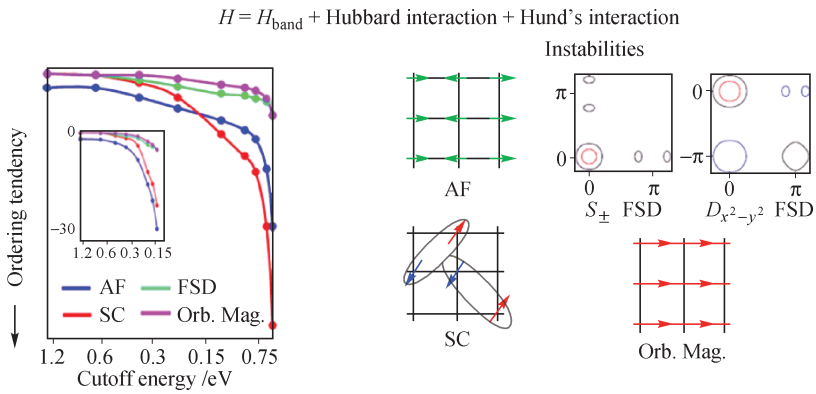


Fig. 8 *Left panel*: A summary of the RG flow of the four leading instabilities for the iron-based superconductors. *Right panels*: The caricatures of the ordering patterns associated with the four electronic instabilities.

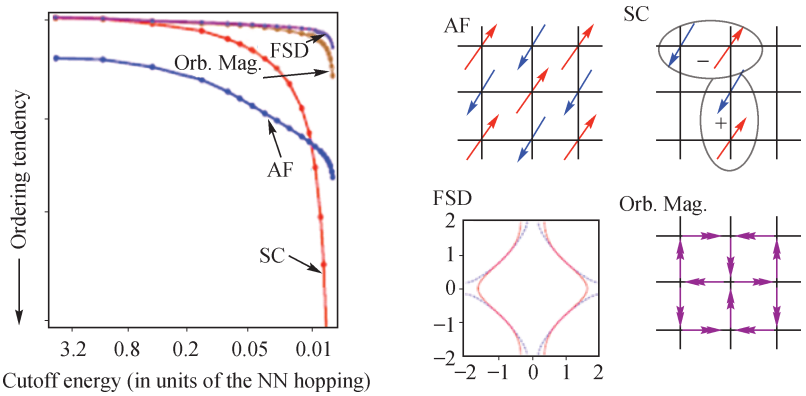


Fig. 9 *Left panel*: A summary of the RG flow of the four leading instabilities for the one-band Hubbard model when the Hubbard U is half the bandwidth. *Right panels*: The caricatures of the ordering patterns associated with the four electronic instabilities.

result holds when the strength of the local correlation varies from half the bandwidth to the full bandwidth. At this point it is important to note that similar FRG results have been obtained by other groups [30, 31].

Interestingly, when we followed Honerkamp and Rice's work on the cuprates [24] in applying the FRG to the single-band Hubbard model, the same set of electronic instabilities, i.e., pairing, antiferromagnetism, Pomeranchuk distortion and bond-current magnetism, were found (Fig. 9). Because FRG requires weak coupling we have chosen the Hubbard U to be only half of the bandwidth. The fact that the same set of electronic instabilities is found in the models for the pnictides and (possibly) the overdoped cuprates is a striking observation. It suggests that these two systems have similar physics. As to the underdoped cuprates, it clearly lies out of the reach of the FRG.

Another indication of the similarity between the cuprate and pnictide physics is encountered when we study the double-layer Hubbard model with a tunable hopping constant t_z [28] (see also Ref. [32]). For small t_z the Fermi surfaces resemble that of the cuprates, and at large t_z the Fermi surface consists of an electron pocket at the Brillouin zone center and a hole pocket at the zone corner. The latter is reminiscent of the electronic structure of the iron-based superconductors (Fig. 11). The doping versus t_z phase diagram obtained from FRG is shown in the mid panel of Fig. 11. For sufficient doping, as a function of increasing t_z the superconducting pairing changes from $d_{x^2-y^2}$ to $S_\pm$. Thus the double layer hubbard model with tunable t_z seems to interpolate between the cuprates and the iron-based superconductors. In both limits what triggers pairing is the umklapp scattering at momentum $2\boldsymbol{Q}$, where $\boldsymbol{Q} = (\pi, \pi)$ is the magnetic ordering wavevector. If one decouples such scattering in the particle–hole channel it leads to antiferromagnetism; on the other hand, if one decouples it in the particle–particle channel one gets sign-changing superconducting pairing. Because the two different decoupling differ by a sign, for both antiferromagnetism and superconducting pairing to gain energy, the order parameter for the latter must change the sign as $\Delta(\boldsymbol{k}) \to \Delta(-\boldsymbol{k} + \boldsymbol{Q})$. In fact,

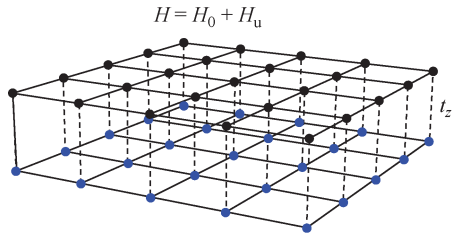


Fig. 10 The double-layer hubbard model with a inter-layer hopping matrix element t_z.

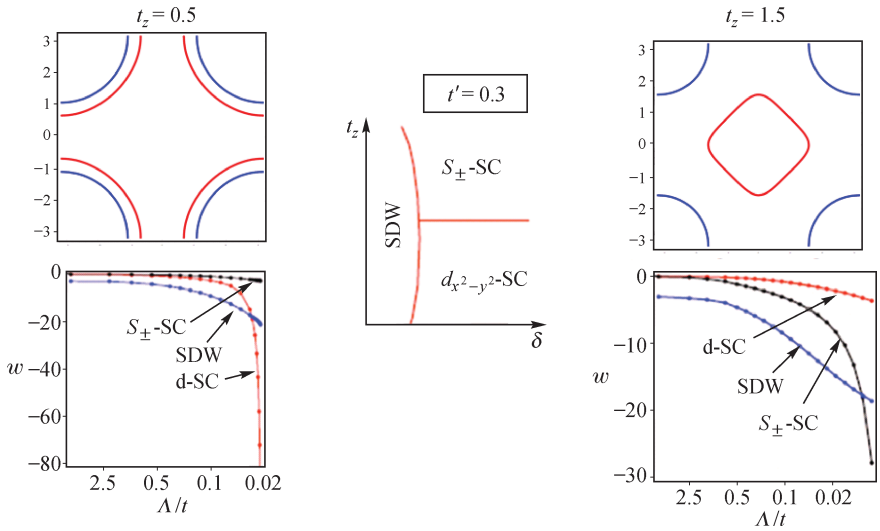


Fig. 11 The Fermi surfaces (top right and top left panels) of the double-layer Hubbard model at different t_z. The doping is assumed to be 8%. Lower right and lower left panels are the associated FRG flows. *Mid panel*: the schematic phase diagram (t' is the second neighbor hopping matrix element.)

the same statement applied to the FRG result for the pnictides and cuprates, except in the former the magnetic ordering wavevector $\boldsymbol{Q}$ is $(\pi, 0)$ or $(0, \pi)$.

In our opinion the fact that there are four competing instabilities before the system enters the superconducting state implies that there does not exist a sufficiently wide energy (temperature) range in which the normal state of the iron-based materials is controlled by the Fermi liquid "unstable fixed point".

Of course the readers might ask what about the weak coupling assumption? Aren't we told that the iron-based superconductors are intermediate-coupling materials? Should the FRG results be trusted for intermediate coupling? Precisely due to these questions we have collaborated with F. Yang in performing a variational Monte Carlo calculation using partially projected wavefunctions [33]. Due to the fact that there are five bands, the necessity to optimize the degree of projection, and the smallness of the superconducting gap compared with the bandwidth and Hubbard and Hund's energy, such calculation is extremely time consuming. It is a feat that Fan Yang was able to do it. We have checked the electronic instabilities including antiferromagnetism, pairing and two types of Fermi surface distortion as suggested by the FRG calculation. Due to the complexity of the variational Monte Carlo we can not afford to use the entire gap function as variational degrees of freedom when looking at pairing. Therefore we have checked the $S_\pm$ $[\Delta(\boldsymbol{k}) = \Delta_0 \cos k_x \cos k_y]$, extended S $[\Delta(\boldsymbol{k}) = \Delta_0(\cos k_x + \cos k_y)]$, d-wave $[\Delta(\boldsymbol{k}) = \Delta_0(\cos k_x - \cos k_y)]$, and trivial S wave $[\Delta(\boldsymbol{k}) = \Delta_0]$. The result is shown in Fig. 12. According to this result the extended S wave has a slightly better energy than $S_\pm$ (the energy difference is similar to the error bar). Thus unlike what is claimed in Ref. [34] the real space next-nearest neighbor pairing is not the best pairing form factor (this of course will change if one adds a second neighbor antiferromagnetic exchange interaction by hand to favor $\Delta(\boldsymbol{k}) = \Delta_0 \cos k_x \cos k_y$). The most likely pairing form factor is a mixture of $S_\pm$ and extended S. Since $(\cos k_x + \cos k_y)$ has nodes on the electron Fermi surfaces, this is likely to introduce substantial gap anisotropy on the electron Fermi surfaces, as predicted by FRG [27, 28, 30, 31, 35]. As to the two types of Fermi surface distortion, the variational Monte Carlo yielded results that agree with the FRG prediction qualitatively. Thus we feel that we have studied the electronic instabilities of the iron-based materials from both the weak and strong coupling point of views and reached qualitatively the same conclusions.

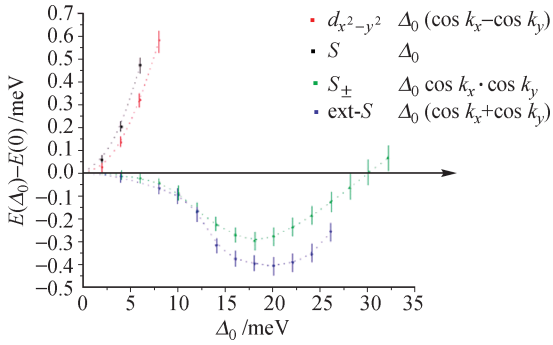


Fig. 12 The variational Monte Carlo results of the energy reduction (per unit cell) of four different pairing form factors (for the pnictides).

To conclude, for conventional superconductors there is a wide crossover range in energy/temperature in which Fermi liquid controls the low energy physics, and Cooper pairing is the only instability. For unconventional superconductors such as the iron-based superconductors, we find multiple competing instabilities in the normal state. Hence the Fermi liquid crossover regime was not found. For both models describing the iron-based materials and

the one-band Hubbard model, we found the same set of electronic instability, suggesting similar underlying electronic scattering mechanism that triggers them. From our study what triggers pairing is the strong umklapp scattering at momentum $2\boldsymbol{Q}$ where $\boldsymbol{Q}$ is the magnetic ordering wavevector(s).

Acknowledgements This review is based on results obtained in collaboration with Hui Zhai and Fan Yang, to whom we are deeply grateful. D. H. Lee acknowledge the support by the DOE grant number DE-AC02-05CH11231.

References

1. J. Bardeen, Physics Today, 1963, 16(1): 19
2. J. Bardeen, L. N. Cooper, and J. R. Schrieffer, Phys. Rev., 1957, 108: 1175
3. L. Landau, Sov. Phys. JETP, 1957, 3: 920
4. This fact has been rephrased in the renormalization group language in R. Shankar, Rev. Mod. Phys., 1994, 66: 129
5. J. Polchinski, Proceedings of 1992 Theoretical Advanced Studies Institute in Elementary Particle Physics, edited by J. A. Harvey, and J. Polchinski, Singapore: World Scientific, 1993
6. C. M. Varma, P. B. Littlewood, S. Schmittrink, E. Abrahams, and A. E. Ruckenstein, Phys. Rev. Lett., 1989, 63: 1996
7. P. A. Lee, N. Nagaosa, and X.-G. Wen, Rev. Mod. Phys., 2006, 78: 17
8. Y. Kamihara, T. Watanabe, M. Hirano, and H. Hosono, J. Am. Chem. Soc., 2008, 130: 3296
9. V. J. Emery and S. A. Kivelson, Phys. Rev. Lett., 1995, 74: 3253
10. N. Doiron-Leyraud, P. Auban-Senzier, S. René de Cotret, C. Bourbonnais, D. Jérome, K. Bechgaard, and L. Taillefer, Phys. Rev. B, 2009, 80: 214531
11. S. A. Kivelson, I. P. Bindloss, E. Fradkin, V. Oganesyan, J. M. Tranquada, A. Kapitulnik, and C. Howald, Rev. Mod. Phys., 2003, 75: 1201
12. J. Zaanen, Nature, 2000, 404: 714
13. S. Chakravarty, R. B. Laughlin, D. K. Morr, and C. Nayak, Phys. Rev. B, 2001, 63: 094503
14. C. M. Varma, Phys. Rev. Lett., 1999, 83: 3538
15. M. Yi, D. H. Lu, J.-H. Chu, J. G. Analytis, A. P. Sorini, A. F. Kemper, B. Moritz, S.-K. Mo, R. G. Moore, M. Hashimoto, W.-S. Lee, Z. Hussain, T. P. Devereaux, I. R. Fisher, and Z.-X. Shen, PNAS, 2011, 108(17): 6878
16. L. W. Harriger, H. Q. Luo, M. S. Liu, C. Frost, J. P. Hu, M. R. Norman, and P. Dai, Phys. Rev. B, 2011, 84: 054544
17. Y. Matsuda et al., to be published
18. S. Raghu, Xiao-Liang Qi, C. Honerkamp, and Shou-Cheng Zhang, Phys. Rev. Lett., 2008, 100: 156401
19. For a review of the electronic structure determined by angle-resolved photoemission spectroscopy, see, e.g., X. J. Zhou, G. D. Liu, H. Y. Liu, L. Zhao, W. T. Zhang, X. W. Jia, and J. Q. Meng, Front. Phys. China, 2009, 4: 427
20. I. I. Mazin, D. J. Singh, M. D. Johannes, and M. H. Du, Phys. Rev. Lett., 2008, 101: 057003
21. Y. Zhang, L. X. Yang, M. Xu, Z. R. Ye, F. Chen, C. He, H. C. Xu, J. Jiang, B. P. Xie, J. J. Ying, X. F. Wang, X. H. Chen, J. P. Hu, M. Matsunami, S. Kimura, and D. L. Feng, Nat. Mater., 2011, 10: 273
22. For theoretical studies of the electronic structure of AFe_2Se_2, see, e.g., F.-J. Ma, Z. Y. Lu, and T. Xiang, Front. Phys. China, 2010, 5(2): 147
23. D. Zanchi and H. J. Schulz, Phys. Rev. B, 2000, 61: 13609
24. C. Honerkamp, M. Salmhofer, N. Furukawa, and T. M. Rice, Phys. Rev. B, 2001, 63: 035109
25. K. G. Wilson and M. E. Fisher, Phys. Rev. Lett., 1972, 28: 240
26. F. Wang, H. Zhai, Y. Ran, A. Vishwanath, and D.-H. Lee, arXiv:0805.3343, 2008
27. F. Wang, H. Zhai, Y. Ran, A. Vishwanath, and D.-H. Lee, Phys. Rev. Lett., 2009, 102: 047005
28. H. Zhai, F. Wang, and D.-H. Lee, Phys. Rev. B, 2009, 80: 064517
29. Jun Zhao, Q. Huang, Clarina de la Cruz, Shiliang Li, J. W. Lynn, Y. Chen, M. A. Green, G. F. Chen, G. Li, Z. Li, J. L. Luo, N. L. Wang, and P. Dai, Nat. Mater., 2008, 7: 953
30. R. Thomale, C. Platt, J. Hu, C. Honerkamp, and B. A. Bernevig, Phys. Rev. B, 2009, 80: 180505(R)
31. R. Thomale, C. Platt, W. Hanke, and B. A. Bernevig, Phys. Rev. Lett., 2011, 106: 187003
32. T. A. Maier and D. J. Scalapino, arXiv:1107.0401, 2011
33. F.Yang, H. Zhai, F. Wang, and D.-H. Lee, Phys. Rev. B, 2011, 83: 134502
34. J. P. Hu and H. Ding, arXiv:1107.1334, 2011
35. F. Wang, H. Zhai, and D.-H. Lee, Europhys. Lett., 2009, 85: 37005